IOP Conf. Series: Materials Science and Engineering **346** (2018) 012074 doi:10.1088/1757-899X/346/1/012074

Study of Surface Roughness and Cutting force in machining for 6068 Aluminium alloy

D. Purushothaman[1], Krishna Kaushik Yanamundra[2], Gokul Krishnan[3], C. Perisamy[4]

[1,2,3,4] Mechanical Engg. Department, BITS Pilani, Dubai Campus

Abstract: Metal matrix composites, in particular, Aluminium Hybrid Composites are gaining increasing attention for applications in air and land because of their superior strength to weight ratio, density and high temperature resistance. Aluminium alloys are being used for a wide range of applications in Aerospace and Automobile industries, to name a few. The Aluminium Alloy 6068 has been used as the specimen. It is mainly composed of Aluminium (93.22 - 97.6 %), Magnesium (0.60 - 1.2 %), Silicon (0.60 - 1.4 %) and Bismuth (0.60 - 1.1 %). Aluminium 6068 is widely used for manufacturing aircraft structures, fuselages and wings. It is also extensively used in fabricating automobile parts such as wheel spacers. In this study, tests for the measurement of surface roughness and cutting force has been carried out on the specimen, the results evaluated and conclusions are drawn. Also the simulation of the same is carried out in a commercial FE software – ABAQUS.

Key words: Surface roughness, cutting force, 6068 Aluminium alloy, lathe, regression model, ABAQUS, FEM.

1. Introduction

6068 Aluminium alloy is an alloy in the wrought Aluminium-Magnesium-Silicon family (6000 or 6xxx series). It is much more closely related to the alloy 6063 than to 6061. The main difference between 6068 and 6063 is that 6063 has a slightly higher magnesium content. It can be formed by extrusion, forging or rolling, but as a wrought alloy it is not used in casting. It cannot be work hardened, but is commonly heat treated to produce tempers with a higher strength but lower ductility [1]. The **Table 1.1** below shows the composition of Aluminium 6068 alloy.

The main aim of this experimental paper is to study, analyze and realize the experimental measurement of cutting forces during machining and surface roughness at turning of rotational parts made from Aluminium alloy 6068.

TABLE 1.1 - Composition of Aluminium Alloy 6068.

Component Elements Properties	Metric
Aluminum, Al	93.22 - 97.6 %
Bismuth, Bi	0.60 - 1.1 %
Chromium, Cr	<= 0.30 %
Copper, Cu	<= 0.10 %
Gallium, Ga	<= 0.03 %
Iron, Fe	<= 0.50 %
Lead, Pb	0.20 - 0.40 %
Magnesium, Mg	0.60 - 1.2 %
Manganese, Mn	0.40 - 1.0 %
Nickel, Ni	<= 0.05 %
Other, each	<= 0.05 %
Other, total	<= 0.15 %
Silicon, Si	0.60 - 1.4 %
Titanium, Ti	<= 0.20 %
Vanadium, V	<= 0.05 %
Zinc, Zn	<= 0.30 %

2. Experiment

The machining was performed on a Lathe machine. A lathe is used to perform various operations such as cutting, sanding, knurling, drilling, or deformation, facing, turning, with tools that are applied to the workpiece to create an object with symmetry about an axis of rotation. When it comes to automobile parts like crankshafts, and camshafts and other symmetric components, Aluminium is machined using Lathes. The experimental results will help in analyzing the mechanical properties for those parts.

2.1 Cutting force during Machining

The Cutting force was measured using a Lathe tool dynamometer. The workpiece is held at the chuck of the lathe with the dynamometer attached to the cutting tool. The **Fig 2.1** below shows a lathe tool dynamometer. It gives the force in the X, Y and Z axes during the machining process. The forces during machining are dependent on depth of cut, feed rate, cutting speed, tool material and geometry, material of the work piece and other factors such as use of lubrication/cooling during machining.

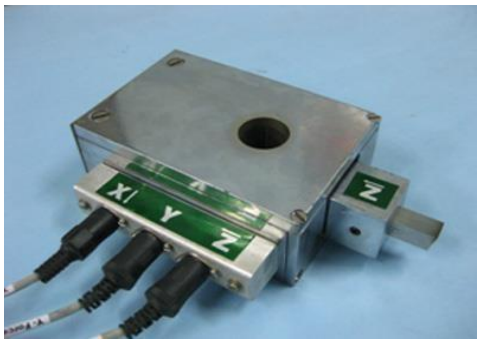

Fig 2.1: lathe tool dynamometer

In this study, the dependence of cutting force in each of the 3 axes with the RPM, Feed rate and Depth of cut is analyzed. The **Table 2.1** below shows the results obtained during the experiment

TABLE 2.1: Cutting force results

			Cutting Force (Kgf)		
RPM	**Feed (mm)**	**Depth of Cut (mm)**	**X Axis**	**Y Axis**	**Z Axis**
160	0.25	0.5	0	7	4
	0.25	1	-1	13	6
	0.25	1.5	-5	21	5
360	0.25	0.5	0	9	4
	0.25	1	-1	11	4
	0.25	1.5	-2	18	6
560	0.25	0.5	0	6	3
	0.25	1	-2	9	5
	0.25	1.5	-2	12	16
160	0.3	0.5	0	4	10
	0.6	0.5	1	6	13
	1	0.5	1	5	3
360	0.3	0.5	0	8	4
	0.6	0.5	1	7	3
	1	0.5	2	15	13
560	0.3	0.5	0	2	1
	0.6	0.5	1	4	3
	1	0.5	2	8	7

2.2 Surface Roughness test after machining

The Surface roughness test was conducted after the machining process was complete. It gives an idea of how the object interacts with the environment. The **Table 2.2** below shows the change in surface roughness at different RPM, Feed and Depth of cut.

TABLE 2.2: Surface Roughness Results

RPM	**Feed (mm)**	**Depth of Cut (mm)**	**Surface Roughness (µm)**
160	0.25	0.5	5.254
	0.25	1	3.827
	0.25	1.5	5.786
360	0.25	0.5	6.422
	0.25	1	5.825
	0.25	1.5	5.308
560	0.25	0.5	3.378
	0.25	1	6.803
	0.25	1.5	4.528
160	0.3	0.5	2.144
	0.6	0.5	5.698
	1	0.5	6.514
360	0.3	0.5	2.326
	0.6	0.5	9.238
	1	0.5	10.214
560	0.3	0.5	2.153
	0.6	0.5	7.615
	1	0.5	7.198

2.3 Regression Model - ANOVA

Regression model: Force along X axis (C4) = -7.8 - 0.0248 C1 + 15.6 C2 + 19.6 C3 + 0.000082 C1*C1 - 2.7 C2*C2 + 13.7 C3*C3 + 0.0133 C1*C2 - 0.0586 C1*C3

C1= Speed; C2= Feed and C3=Depth of cut

Analysis of Variance

Source	DF	Adj SS	Adj MS	F-Value	P-Value
Regression	3	13.8662	4.6221	8.40	0.002
C1	1	0.0833	0.0833	0.15	0.703
C2	1	3.7769	3.7769	6.86	0.020
C3	1	13.6847	13.6847	24.87	0.000
Error	14	7.7032	0.5502		
Total	17	21.5694			

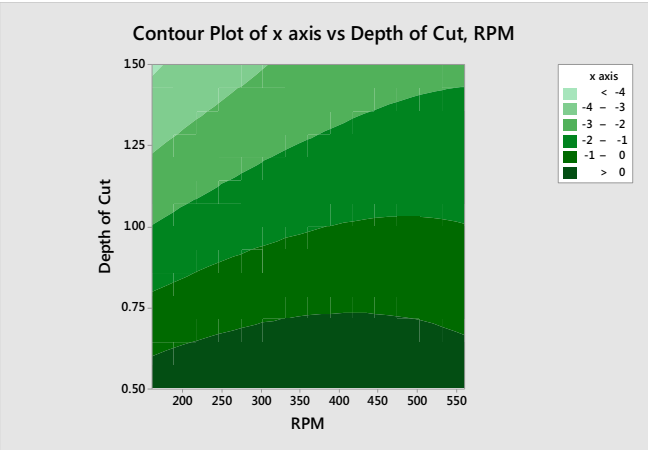

Fig 2.2: contour plot of force along x axis vs speed and depth of cut

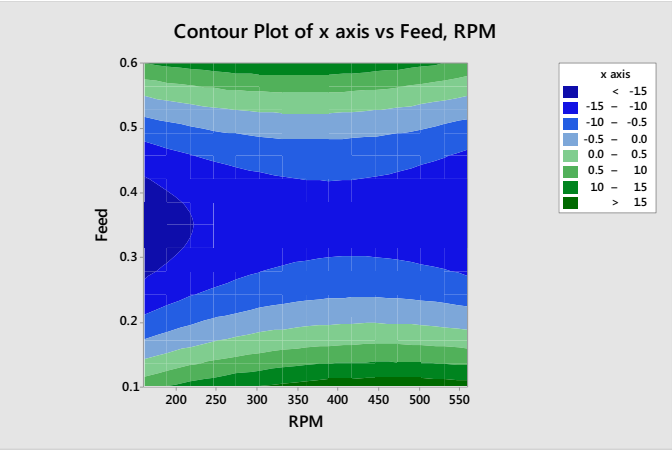

Fig 2.3: contour plot of force along x axis vs speed and feed

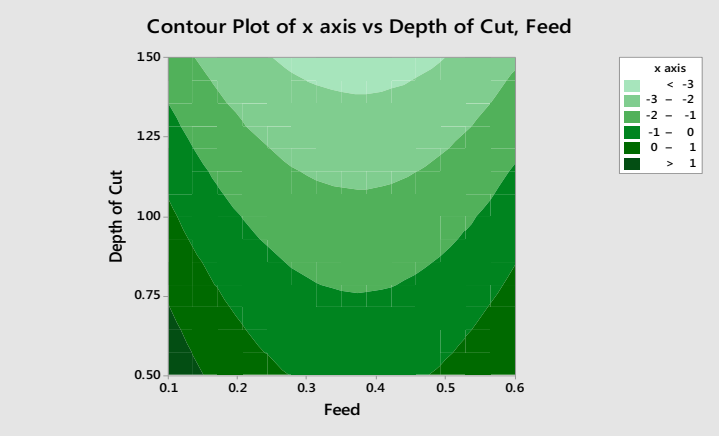

Fig 2.4: contour plot of force along x axis vs feed and depth of cut

Force along Y axis (C5) = -2.23 + 0.0588 C1 - 22.1 C2 + 11.3 C3 - 0.000081 C1*C1 + 17.2 C2*C2 + 2.65 C3*C3 + 0.0130 C1*C2 - 0.01643 C1*C3

Analysis of Variance

Source	DF	Adj SS	Adj MS	F-Value	P-V
Regression	3	300.59	100.198	10.63	0.001
C1	1	18.75	18.750	1.99	0.180
C2	1	19.34	19.343	2.05	0.174
C3	1	270.57	270.567	28.72	0.000
Error	14	131.91	9.422		
Total	17	432.50			

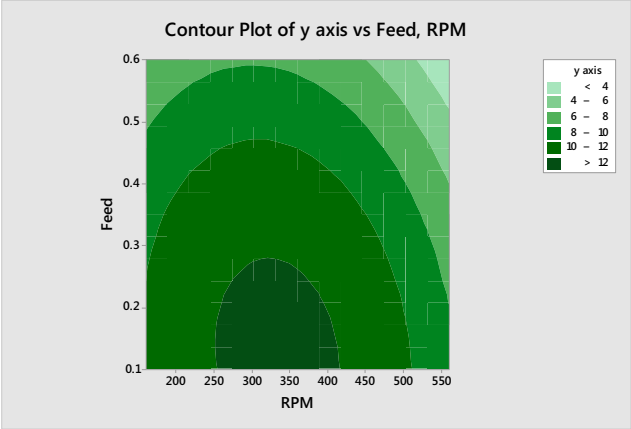

Fig 2.5: contour plot of force along y axis vs speed and feed

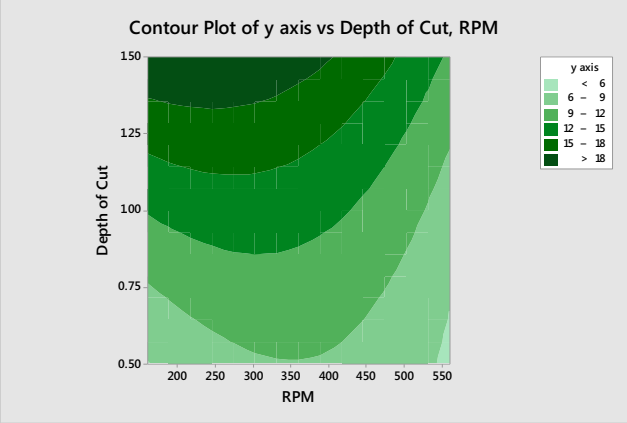

Fig 2.6: contour plot of force along y axis vs speed and depth of cut

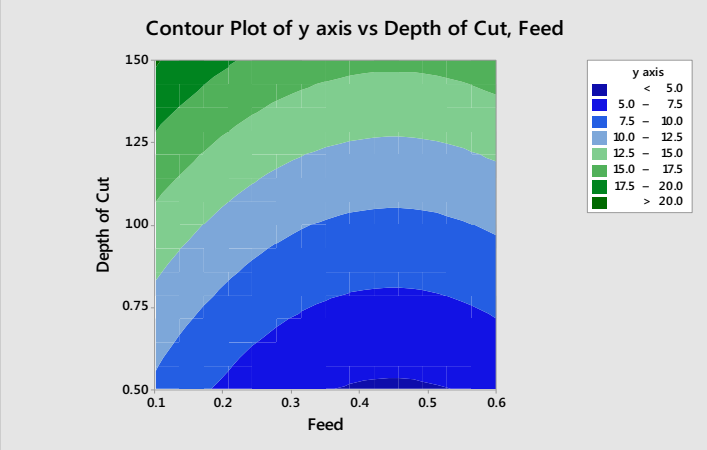

Fig 2.7: contour plot of force along y axis vs feed and depth of cut

Regression model:

Force along Z axis (C6) = 22.5 - 0.0593 C1 + 1.2 C2 - 23.0 C3 + 0.000017 C1*C1 - 5.2 C2*C2 + 6.1 C3*C3 + 0.0278 C1*C2 + 0.0434 C1*C3

Analysis of Variance

Source	DF	Adj SS	Adj MS	F-Value	P-V
Regression	3	52.456	17.485	1.01	0.416
C1	1	3.000	3.000	0.17	0.683
C2	1	30.789	30.789	1.79	0.203
C3	1	40.377	40.377	2.34	0.148
Error	14	241.322	17.237		
Total	17	293.778			

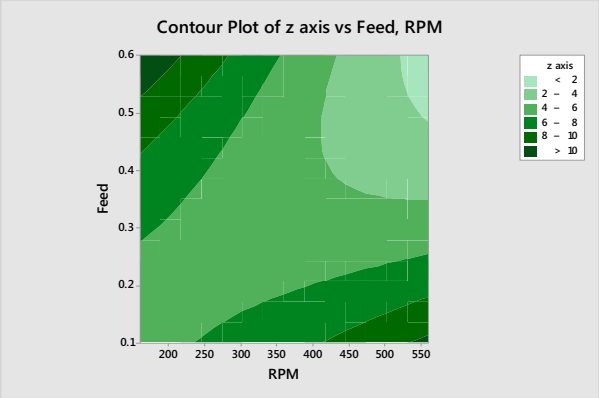

Fig 2.8: contour plot of force along z axis vs speed and feed

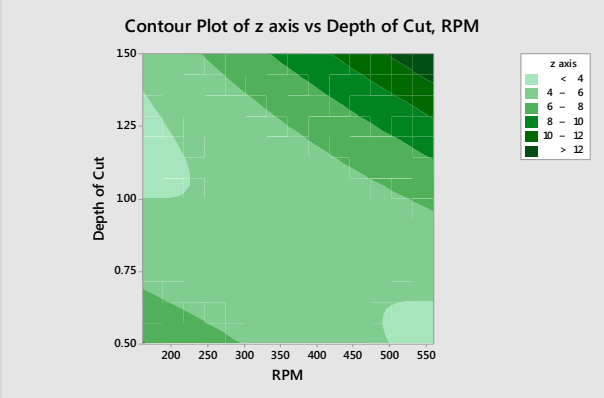

Fig 2.9: contour plot of force along z axis vs speed and depth of cut

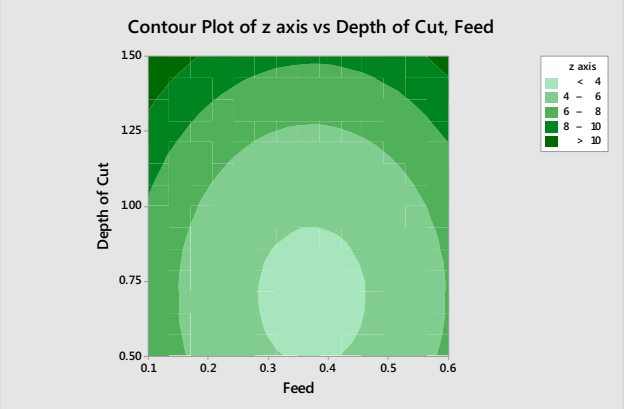

Fig 2.10: contour plot of force along z axis vs feed and depth of cut

Surface Roughness, (micro meter) = -8.37 + 0.0258 C1 + 17.3 C2 + 10.8 C3 - 0.000037 C1*C1 - 10.10 C2*C2 - 4.57 C3*C3 + 0.0039 C1*C2 + 0.00020 C1*C3

Analysis of Variance

Source	DF	Adj SS	Adj MS	F-Value	P-V
Regression	3	39.5603	13.1868	3.80	0.035
C1	1	0.5010	0.5010	0.14	0.710
C2	1	38.5031	38.5031	11.09	0.005
C3	1	4.5132	4.5132	1.30	0.273
Error	14	48.5925	3.4709		
Total	17	88.1528			

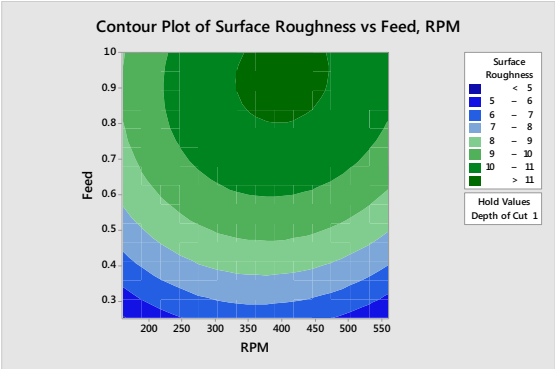

Fig 2.11: contour plot of surface roughness vs speed and feed

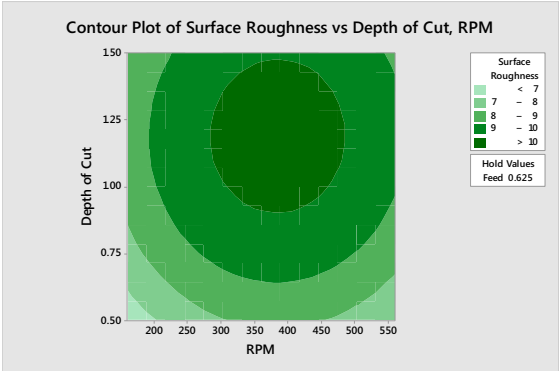

Fig 2.12: contour plot of roughness vs speed and depth of cut

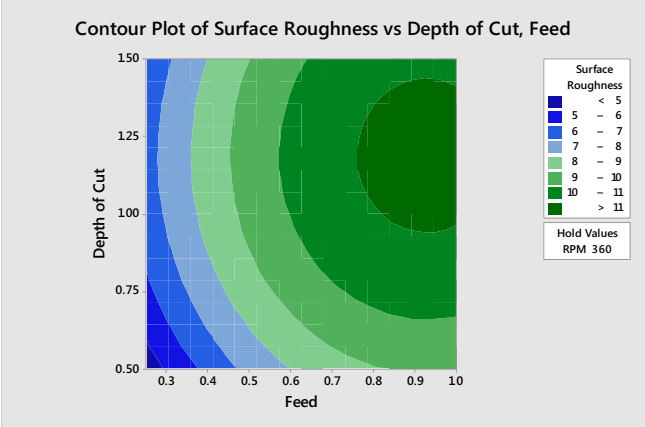

Fig 2.13: contour plot roughness vs feed and depth of cut

2.4 FEM Simulation

The model has been created in ABAQUS and approximated as a flat surface machining and a dynamic/explicit analysis has been carried out on the model. The material model is defined according to the Johnson cook model and the damage evolution has also been given. The speed of the tool has been varied by adjusting the time interval. The feed is manipulated by adjusting the width of the slab and the depth of cut is defined as is. The conditions similar to experimental conditions are assigned and the results are obtained.

3. Results and discussion

The figure **Fig 3.1** below shows the variation in surface roughness when the Depth of cut is kept constant for various RPM and Feed (Feed in the X-Axis and Roughness in the Y-axis with different color representing different speeds RPM).

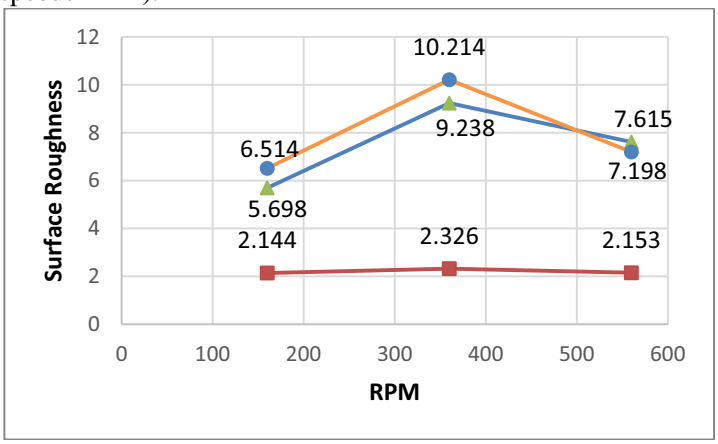

Fig 3.1: roughness vs speed

The above graph depicts the strength of the material with respect to different RPM at constant feed. It is noted that, at 560RPM, the roughness value is 6.803. At 160RPM for the same feed, the roughness value is 3.827. Hence it is clear that with increase in RPM, the roughness value increases. Hence the wear behavior of the material also gets affected. For 360RPM, there is a gradual decrease in the roughness value when feed is kept constant. Hence it is evident that with increase in feed, the wear behavior gets affected. The wear behavior is inversely proportional to feed and RPM, when depth of cut is kept constant.

The figure **Fig 3.2** below shows the variation in the surface roughness when the Feed is kept constant for varying RPM and Depth of cut (Depth of cut in the x-Axis and Roughness in the Y-axis with different color representing different speeds in RPM).

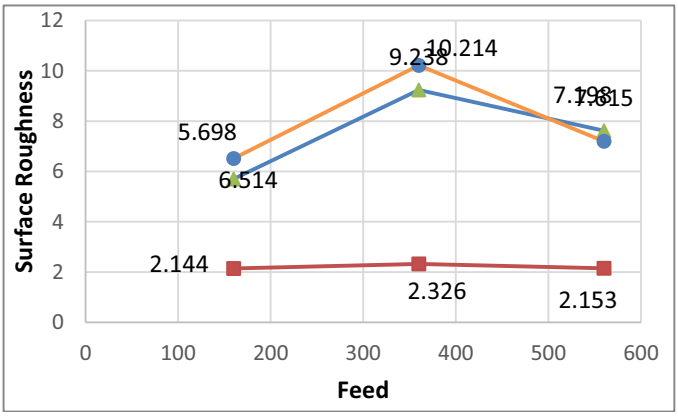

Fig 3.2: roughness vs depth of cut

The feed is kept constant; depth of cut is varied for the same RPM values and the roughness number is noted. It is clear from the graph that with increase in RPM, there is an increase in roughness number. At a lower depth of cut, Roughness value at the 3 RPM levels averages up to 2.207. This value can be taken for all the three cases. At higher depth of cut, there is a decent rise in the roughness value. For 560RPM, with increase in depth of cut, there is a slight decrease in the roughness value. This indicates that when we vary depth of cut w.r.t the RPM, at higher RPM the roughness value tends to be constant.

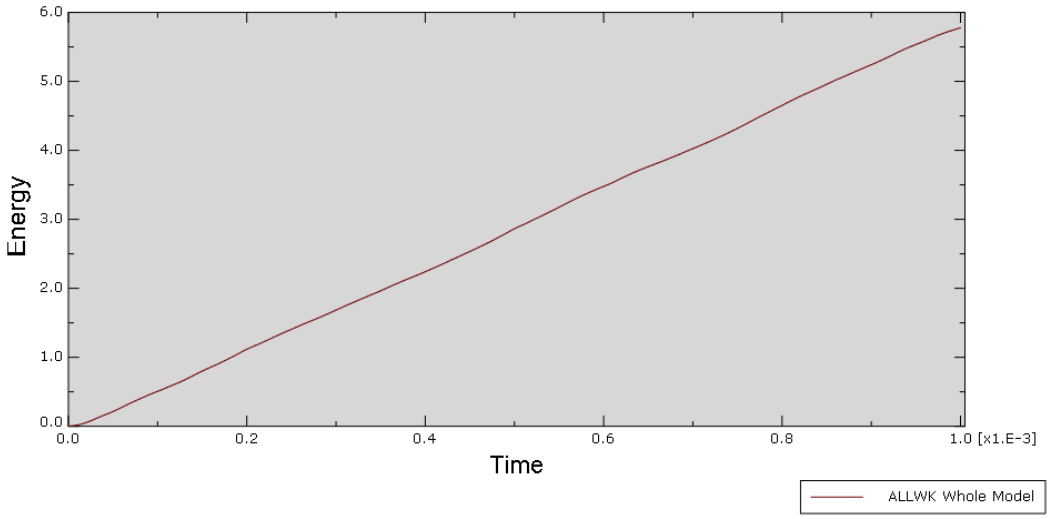

Fig 3.3 : ALLWK plot of the simulated model depicting external work.

ALLWK plot helps us to find the final forces acting on the workpiece when differentiated across the length of the workpiece. The contour plots of the mises components in the workpiece are depicted in fig 3.5 and the stresses in 1, 2 and 3 directions along the time axis are depicted in the plot in fig 3.4

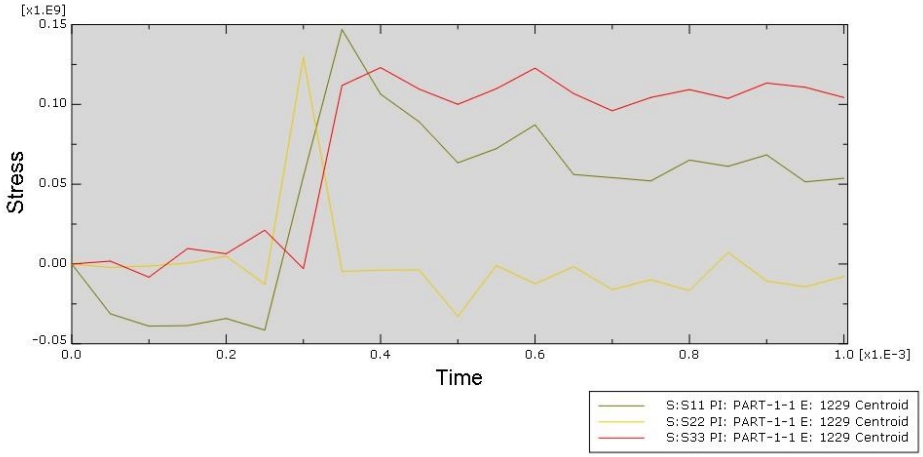

Fig 3.4: Stress vs time at centroid of a picked element set.

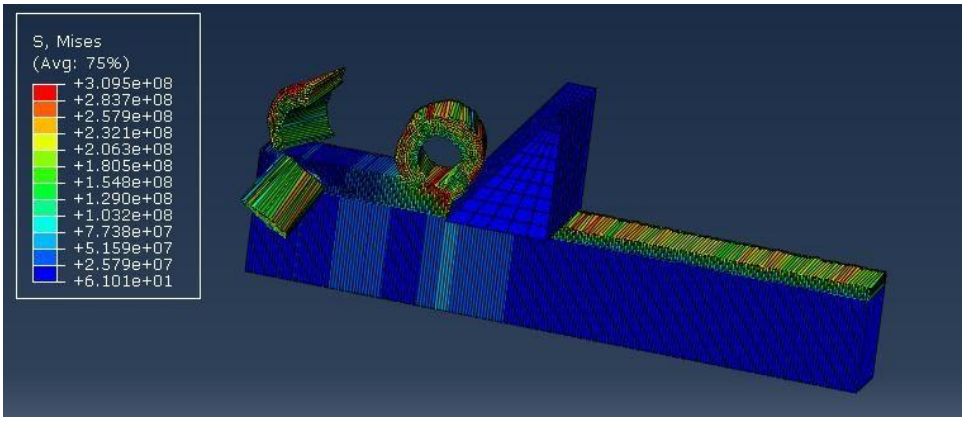

Fig 3.5: Stresses in the body while machining contour plot

Note the type of chip formation in Fig 3.5 and this will vary as the speed varies. When the Forces are plotted the following results are obtained as shown in Fig 3.6. These observations during the simulations can be correlated with the experimental results. Also Contact shear and normal forces are also plotted in Fig 3.7.

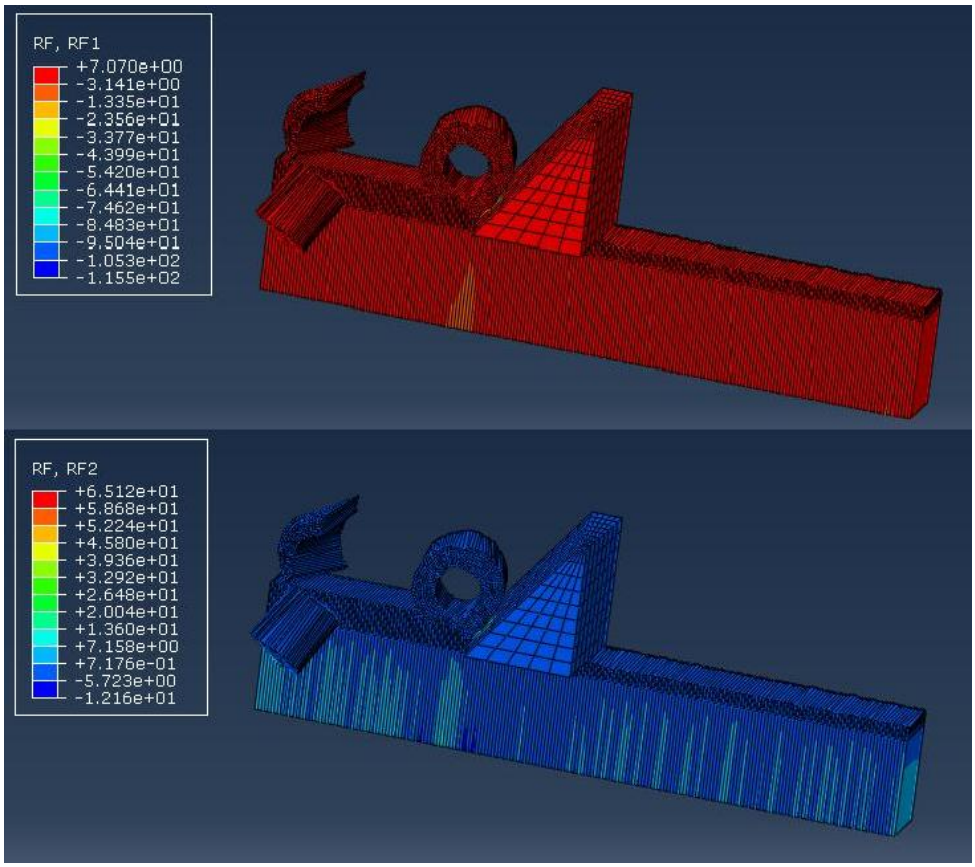

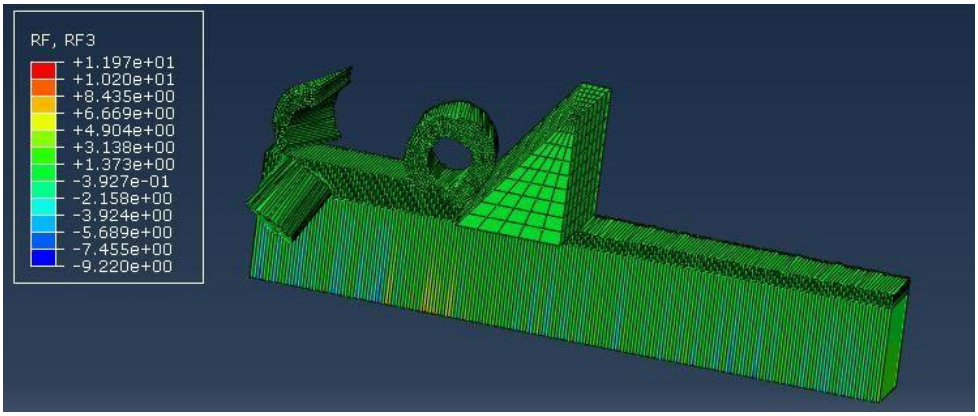

Fig 3.6: Forces in x, y and z directions

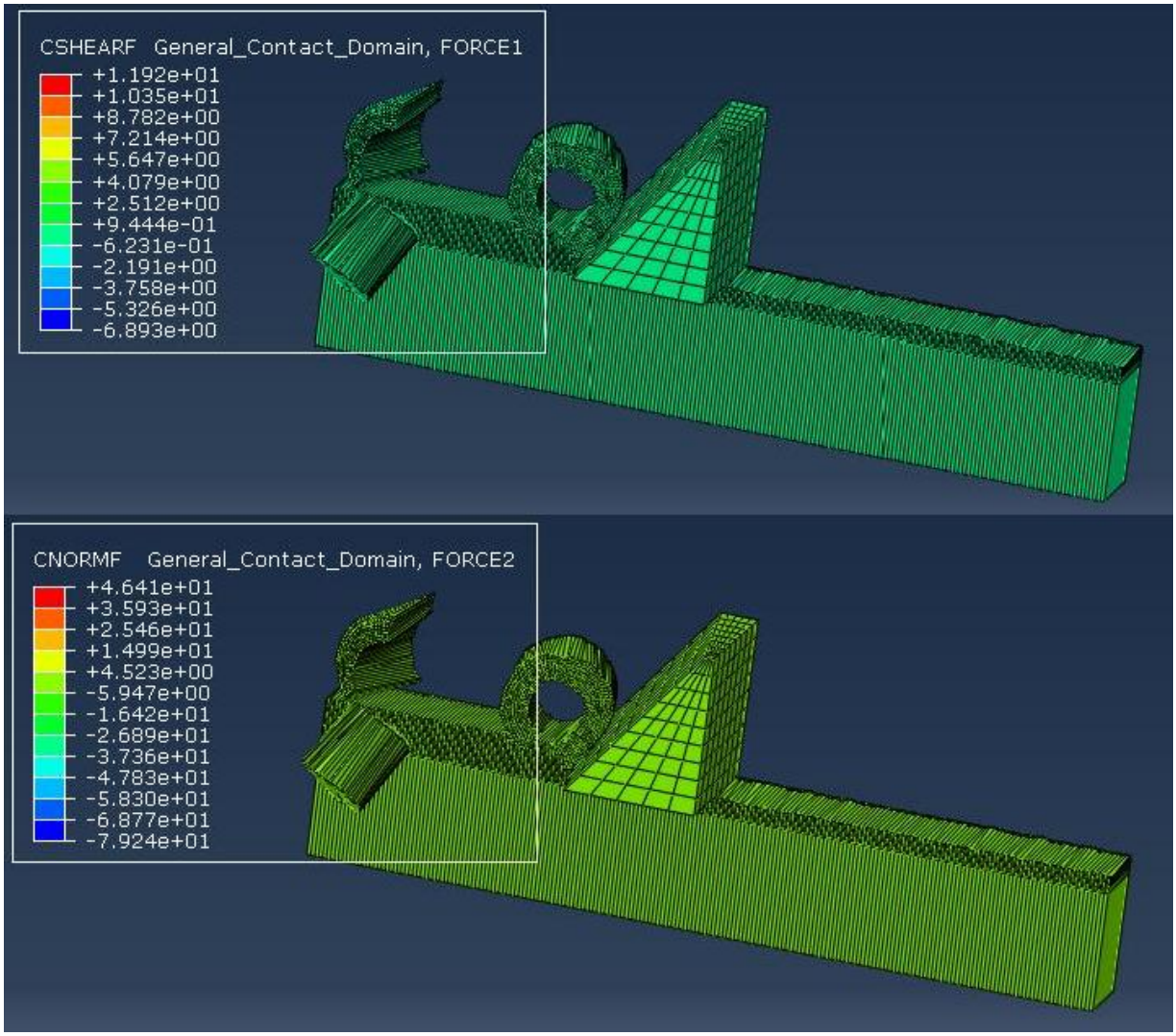

Fig 3.7: Shear and Normal Contact forces.

4. Conclusion

Aluminium 6082 is an alloy of various other elements. This type of alloy has a specific strength and wear-behavior, which has been explained in the literature review section. Using Lathe tool dynamometer the cutting force was noted with respect to the co-ordinates. These co-ordinates at each axis vary due to the increase and decrease of RPM, feed rate, and cutting feed in each of the above mentioned cases. From the table, Cutting force is maximum when the feed increases keeping the depth of cut constant, and vice versa. With increases in cutting force and rpm, the wear rate decreases. With increase in RPM and feed, the roughness value decreases. This is a prime factor to determine the strength of the material with respect to the feed rate. Higher the feed rate, higher the roughness value, more the wear rate of the material. Al-6068 is a standard alloy that has various. Here, the material wear rate is expected to increase when depth of cut and feed are varied.

REFERENCES

[1] Wu Changlin, Heyan D, and Yi C. "Surface roughness prediction for aluminum alloy wheel surface polishing using a PSO-based multilayer perceptron." Intelligent Systems and Applications, 2009. ISA 2009. *International Workshop on. IEEE, 2009.Strunk, W., Jr., & White, E. B. (1979). The elements of style* (3rd ed.). New York: MacMillan.

[2] Venkatesan K., et al. "Study of cutting force and surface roughness in machining of Al alloy hybrid composite and optimized using response surface methodology." *Procedia Engineering 97* (2014): 677-686.

[3] Sharma S C, Girish B M, Kamath R and Satish B M,1999, “Fractography, fluidity, and tensile properties of aluminum/hematite particulate composites”, *Journal of Materials Engineering and Performance*, Vol.8, No. 3, pp.309-314.

[4] Seah K H W, Sharma S C, Rao P R and B M Girish B M, 1995, “Mechanical properties of ascast and heat-treated ZA-27/silicon carbide particulate composites”, *J.Materials and Design,*Vol.16, Issue 5, pp.277-281.

[5] Shanta S, Krishna M and Jayagopal U, 2001, “A study on damping behaviour of aluminite particulate reinforced ZA-27 alloy metal matrix composites”, *J. of Alloys and Compounds*, Vol.314, Issue1-2, pp.268-274.

[6] Natarajan N, Vijayarangan S, Rajendran I, 2007, “ Fabrication,testing and thermal analysis of metal matrix composite brake drum”, *Internal journal of Vehicle Design*, Vol.44, No-3-4, pp.339359.

[7] Prasad S V, Asthana R, 2004, “Aluminiummetal matrix composites for automotive applications: tribological considerations”, *Tribology*, vol.17, No.3, pp.445-453.

[8] Jasmi H, 2001, “The production of cast Metal matrix composite by a modified stir casting method”, *Journal Technology*, 35 (A), pp.9-20.